

This article was downloaded by:

On: 29 January 2011

Access details: *Access Details: Free Access*

Publisher *Taylor & Francis*

Informa Ltd Registered in England and Wales Registered Number: 1072954 Registered office: Mortimer House, 37-41 Mortimer Street, London W1T 3JH, UK



Supramolecular Chemistry

Publication details, including instructions for authors and subscription information:

<http://www.informaworld.com/smpp/title~content=t713649759>

Fluorescence Energy Transfer Study of Interstrand DNA Cross-linking Caused by Rigid Bisintercalator

Bernard Juskowiak^a; Elzbieta Galezowska^a; Teruhisa Ichihara^b; Shigeori Takenaka^b; Makoto Takagi^b; Kenichi Yoshikawa^c

^a Department of Analytical Chemistry, Faculty of Chemistry, A. Mickiewicz University, Poznan, Poland ^b Department of Applied Chemistry, Faculty of Engineering, Kyushu University, Fukuoka, Japan ^c Department of Physics, Faculty of Science, Kyoto University, Kyoto, Japan

Online publication date: 29 October 2010

To cite this Article Juskowiak, Bernard , Galezowska, Elzbieta , Ichihara, Teruhisa , Takenaka, Shigeori , Takagi, Makoto and Yoshikawa, Kenichi(2002) 'Fluorescence Energy Transfer Study of Interstrand DNA Cross-linking Caused by Rigid Bisintercalator', *Supramolecular Chemistry*, 14: 6, 477 – 485

To link to this Article: DOI: 10.1080/1061027021000052689

URL: <http://dx.doi.org/10.1080/1061027021000052689>

PLEASE SCROLL DOWN FOR ARTICLE

Full terms and conditions of use: <http://www.informaworld.com/terms-and-conditions-of-access.pdf>

This article may be used for research, teaching and private study purposes. Any substantial or systematic reproduction, re-distribution, re-selling, loan or sub-licensing, systematic supply or distribution in any form to anyone is expressly forbidden.

The publisher does not give any warranty express or implied or make any representation that the contents will be complete or accurate or up to date. The accuracy of any instructions, formulae and drug doses should be independently verified with primary sources. The publisher shall not be liable for any loss, actions, claims, proceedings, demand or costs or damages whatsoever or howsoever caused arising directly or indirectly in connection with or arising out of the use of this material.

Fluorescence Energy Transfer Study of Interstrand DNA Cross-linking Caused by Rigid Bisintercalator

BERNARD JUSKOWIAK^{a,*}, ELZBIETA GALEZOWSKA^a, TERUHISA ICHIHARA^b, SHIGEORI TAKENAKA^b, MAKOTO TAKAGI^b and KENICHI YOSHIKAWA^c

^aDepartment of Analytical Chemistry, Faculty of Chemistry, A. Mickiewicz University, Grunwaldzka 6, 60-688 Poznan, Poland

^bDepartment of Applied Chemistry, Faculty of Engineering, Kyushu University, Fukuoka 812-81, Japan; ^cDepartment of Physics, Faculty of Science, Kyoto University, Kyoto 606-8502, Japan

(Received 12 January 2001)

The intermolecular cross-linking of DNA with a rigid bisintercalator, 1,4-bis((*N*-methylquinolinium-4-yl)vinyl)benzene (pMQVB) has been studied using fluorescence resonance energy transfer (FRET), fluorescence anisotropy measurements, and dynamic fluorescence microscopy. Short DNA duplexes, single-labeled with fluorescein (donor) and *x*-rhodamine (acceptor), were used as energy transfer partners. Due to the quenching effect of pMQVB on the emission of both fluorescein and *x*-rhodamine, the energy transfer was monitored using the corrected Stern–Volmer plots. The cross-linking ability of pMQVB depended on the ligand structure; the planar *E,E* isomer cross-linked DNA contrary to the non-planar *E,Z* isomer. Dynamic fluorescence microscopy observation also demonstrated the ability of pMQVB to cross-link large T4 DNA molecules.

Keywords: Bisintercalators; Cross-linking; DNA; Fluorescence energy transfer

INTRODUCTION

Most experimental data reported on the interaction of DNA with bisintercalators have been discussed in terms of the intramolecular binding (intercalation sites on the same DNA duplex) [1–3]. Generally, it is explained by the structural properties of the common bisintercalators featured by two intercalating moieties linked by a flexible connector. However, there are a few examples of intercalating ligands reported to exhibit the interstrand cross-linking abilities. Luzopeptin, an antitumor antibiotic containing two substituted quinoline rings linked by a cyclic peptide spacer is the first example in

which interstrand bisintercalation has been evidenced [4]. Lowe *et al.* reported the cross-linking of DNA by the ligands containing intercalating units (phenanthridinium and acridinium) linked by a rigid connector [5,6]. Using ligation assay with linearized plasmid DNA, they separated ligation products: catenates and molecular knots, thus providing evidence for DNA cross-linking. Experiments showed extremely low efficiency of knot production, but the authors observed a significant unwinding of DNA by the ligands. Although DNA binding properties of these ligands had not been studied yet, the authors concluded that undoubtedly ligands interact with DNA by intercalation.

Development of a facile assay able to prove intermolecular bisintercalation is a special problem. Formal proof could be obtained using X-ray crystallography or NMR spectroscopy; other techniques, including analysis of mobility of DNA–bisintercalator products [4] or ligation assay [5,6] have been proved difficult and affected by many limitations (e.g. inhibition of ligase action at higher ligand concentration). Therefore, we decided to develop an alternative assay that exploits the fluorescence resonance energy transfer (FRET), the method that has been successfully applied to study structural and dynamic properties of nucleic acids [7–10]. The idea behind our assay is to apply two single-labeled DNA duplexes, one labeled with a donor, and the other with an acceptor molecule. In the absence of the cross-linking ligand, no FRET signal occurs since both duplexes are randomly distributed in solution,

*Corresponding author. Address: Department of Analytical Chemistry, Faculty of Chemistry, A. Mickiewicz University, Grunwaldzka 6, 60-780 Poznan, Poland. E-mail: juskowia@main.amu.edu.pl

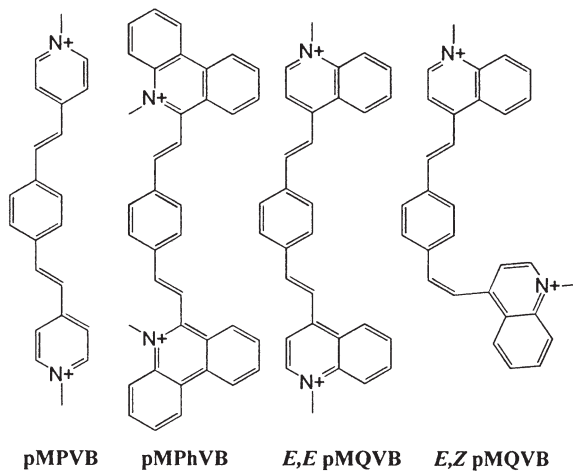


FIGURE 1 Structures of bis(arylvinyl)benzene ligands.

with the separation distance between donor and acceptor far exceeding the Förster critical radius (R_0). Addition of a bisintercalator causes the interstrand cross-linking of duplexes with different labels introducing a spatial organization of the labels. The separation distance of energy transfer partners depends on the length of DNA duplexes and the site of intercalation on particular duplexes. The FRET efficiency depends on the inverse of the sixth power of the distance between the dyes, therefore, the acceptor must be within 10–75 Å from the donor to get a reasonable energy transfer signal; the exact range depending on the spectral properties of the dyes used. The extent of FRET can be measured because the fluorescence of the donor decreases and that of the acceptor increases or becomes “sensitized” with the energy transfer. The addition of the third component (cross-linking ligand) to the donor/acceptor system may cause, however, some problems. Intercalators are commonly featured with extended aromatic systems and exhibit specific spectral characteristics in the visible range. Thus, the cross-linking ligand bands may overlap those of the donor and acceptor. For example, Lowe’s bisintercalator pMPhVB (Fig. 1), proved to be a cross-linking ligand [5], appears to be of less utility for the FRET study because of a significant overlap of its fluorescence band with the emission spectra of fluorescein and α -rhodamine.

Recently, we have studied the DNA binding properties of bis(vinylpyridinium)benzene ligands belonging to the same series as some Lowe’s cross-linking ligands [11]. Our study revealed that pMPVB (Fig. 1) preferred groove binding at AT steps, however, intercalation was observed for GC-rich sequences, and the binding affinity in the latter case was much lower [11]. Another interesting feature of bis(arylvinyl)benzene ligands is their feasibility to undergo photoisomerization. The planar *E,E* isomer, dominant (>95%) in the non-irradiated solution of a

free dye, can be reversibly converted into the non-planar *E,Z* form when exposed to visible light as evidenced by HPLC, NMR, and UV spectroscopies [11,12]. The model of interaction of both the isomers with DNA has been proposed, where only a part of the dye molecule including one of the vinylpyridinium arms was assumed to interact strongly with DNA (minor groove at AT sequences or intercalation pocket at GC steps). The other vinylpyridinium arm sticking out from the DNA groove could undergo *trans*–*cis* isomerization without any dramatic effects on the binding equilibria [11]. If one assumes that this free arm can intercalate into another DNA molecule only in the case of *E,E* isomer, thus producing cross-linked species, *E,Z* isomer can serve as an excellent reference ligand in the cross-linking studies. Pyridinium rings in pMPVB seem to be, however, too small to provide efficient bisintercalation, i.e. cross-linking of DNA. One can expect that their replacement with quinolinium moieties can change the binding preferences of this new ligand, probably enhancing the intercalative binding. Indeed, the quinolinium derivative (pMQVB in Fig. 1) is a potent DNA ligand that binds by intercalation to both GC and AT sites, with binding constants of 4.7×10^6 and $2.4 \times 10^6 \text{ M}^{-1}$, respectively [13]. A preliminary FRET study revealed that pMQVB is able to cross-link DNA [14].

In this work, we report detailed results of the FRET study of the DNA interstrand cross-linking ability of 1,4-bis((*N*-methylquinolinium-4-yl)vinyl)benzene using 8-mer DNA duplexes labeled at the 5’ end with fluorescein (donor) or α -rhodamine (acceptor). Steady-state fluorescence and anisotropy measurements have been carried out. Fluorescence microscopy observations of single T4 DNA molecules also have been performed.

RESULTS AND DISCUSSION

Spectral Properties of Energy Transfer Components

Both labeled oligonucleotides were able to bind to their complementary sequence. Thermal melting temperatures (T_m) were insensitive to the label properties. Both dsONF and dsONXR duplexes gave very similar melting profiles and were marginally less stable ($T_m = 37^\circ\text{C}$) when compared to the corresponding unlabeled DNA ($T_m = 39^\circ\text{C}$). To avoid dissociation of duplexes, all energy transfer measurements were performed at 10°C . The spectral characteristics of the labels were slightly affected by conjugation to oligonucleotides. The maxima of the absorption bands were red shifted *ca.* 3–5 nm and molar absorptivities were slightly lower when compared to the free labels (e.g. $\epsilon^{497} = 6.2 \times 10^4$ and $\epsilon^{493} = 7 \times 10^4 \text{ M}^{-1} \text{ cm}^{-1}$ for ONF and free dye,

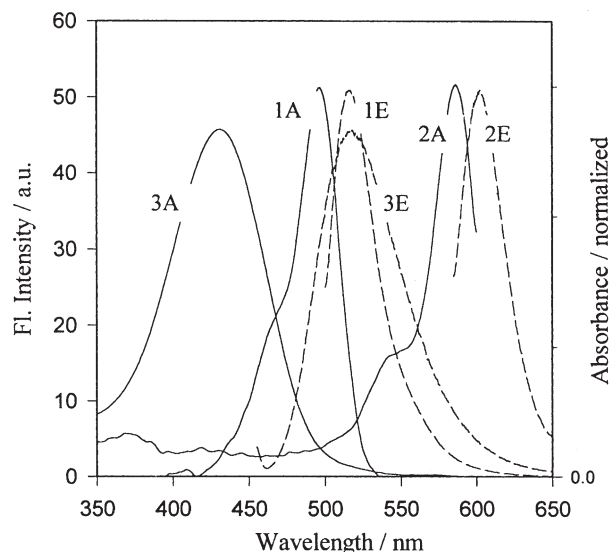


FIGURE 2 Spectral characteristics of the energy transfer components: dsONF (spectra 1A and 1E), dsONXR (spectra 2A and 2E), pMQVB (spectra 3A and 3E). The absorption (A: solid line) and fluorescence spectra (E: broken line) were normalized for display purposes.

respectively). The spectroscopic properties of these dyes are usually influenced by conjugation to oligonucleotides, and dependent on experimental conditions, such as pH, ionic strength, and temperature [7–9]. Figure 2 shows the absorption and fluorescence spectra of ONF and ONXR duplexes as well as the spectra of the cross-linking ligand *E,E* pMQVB. Fluorescein can be nearly selectively excited at 490 nm giving emission centered around 520 nm with a minor contribution from rhodamine emission at 600 nm. Energy transfer should be manifested by quenching of the fluorescein band at 520 nm accompanied by a sensitized emission of rhodamine around 600 nm. The cross-linking ligand pMQVB possesses an absorption band at 440 nm, whose long-wavelength shoulder is supposed to absorb some light ($\lambda_{\text{ex}} = 490 \text{ nm}$), which can lead to the appearance of residual fluorescence signal overlapping the fluorescein emission band at 520 nm. This effect can disturb the detection of spectral changes caused by the energy transfer phenomenon and needs to be taken into account.

Fluorescence Energy Transfer Studies

The fluorescein/rhodamine pair has been widely applied as a donor/acceptor system in energy transfer studies. Both fluorophores have been reported to have a high molar absorptivity and a large quantum yield. This donor/acceptor pair has an appreciable spectral overlap between the emission and absorption spectra of fluorescein and x-rhodamine, respectively. Additionally, there are no reports suggesting their interaction with DNA by

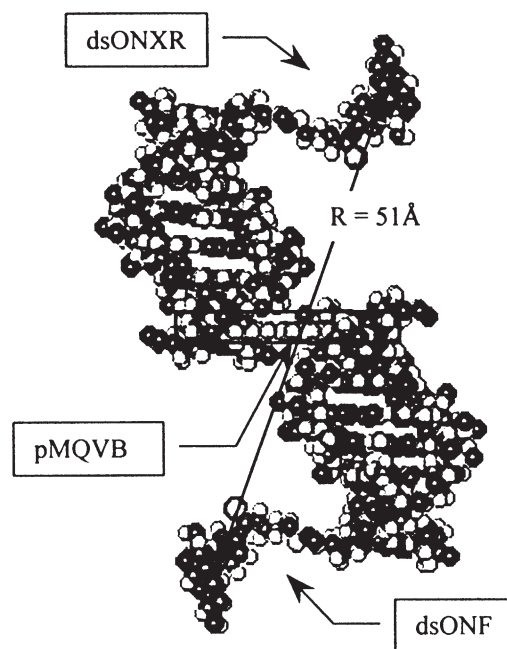


FIGURE 3 A CPK model of 8-mer DNA duplexes single-labeled with fluorescein (dsONF) and x-rhodamine (dsONXR) cross-linked by *E,E* pMQVB. Fluorescein and x-rhodamine serve as a donor/acceptor pair for the resonance energy transfer.

intercalation, groove binding, or other mechanisms, although some quenching effects of DNA have been reported [9]. The Förster critical radius, ($R_0 = 50 \text{ \AA}$) has been calculated assuming a value of 2/3 for the orientation factor κ^2 , $n = 1.36$, and $\phi_{\text{ONF}} = 0.5$ [8,9]. The limiting distance value between donor and

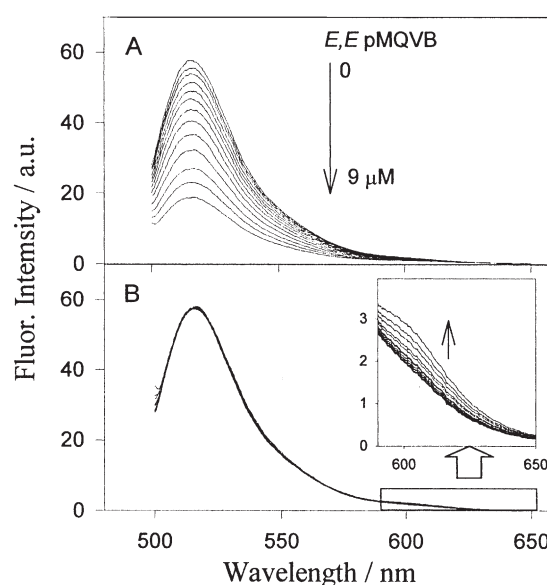


FIGURE 4 Fluorescence titration of dsONF/dsONXR mixture (1:1) with *E,E* pMQVB. Experimental emission spectra (panel A) and after normalization at the maximum of emission of fluorescein (panel B). The inset shows a magnified fragment of the spectrum in which the enhancement of x-rhodamine emission proves the occurrence of the energy transfer process. Conditions: [dsONF] = [dsONXR] = $0.5 \mu\text{M}$, [pMQVB] = $0\text{--}9 \mu\text{M}$, [NaCl] = 200 mM , TE buffer (10 mM , pH 7.8). Excitation wavelength = 490 nm .

TABLE I Values of quenching constants (K_{SV}) and association constants (K_a) of labeled DNA 8-mers/pMQVB systems (mean values \pm s.d. of three determinations)

DNA	200 mM NaCl (<i>E,E</i> pMQVB)		$K_{SV} \times 10^{-5}$ (M^{-1}), 50 mM NaCl*	
	$K_{SV} \times 10^{-5}$ (M^{-1})	$K_a \times 10^{-5}$ (M^{-1})	<i>E,E</i> pMQVB	<i>E,Z</i> pMQVB
dsONXR	3.1 ± 0.5	1.3 ± 0.3	14 ± 3	6.7 ± 1.5
dsONF	14 ± 2	2.6 ± 0.7	36 ± 5	24 ± 4
ssONF	5.9 ± 0.8	—	—	—

* K_{SV} values obtained from the linear parts of upward curved Stern–Volmer plots.

acceptor after cross-linking of two duplexes has been estimated to be *ca.* 51 Å using computer modeling with the 8-mer duplex corresponding to an idealized B-form helix. An assumption was made that pMQVB cross-links both duplexes by intercalation of its quinolinium rings at the unlabeled terminal GC sequences of duplexes (Fig. 3). The intercalation can also take place at other sites, but then it leads to an even smaller separation distance and higher energy transfer efficiency.

The set of emission spectra obtained during the titration of 1:1 molar mixture of dsONF and dsONXR with bisintercalator *E,E* pMQVB is shown in Fig. 4 (panel A). The observed quenching of the donor emission is too large to be accounted for by the energy transfer process exclusively. Moreover, the expected sensitized emission of the acceptor at about 600 nm cannot be clearly detected. An explanation of the observed spectral changes should take into regard the quenching properties of pMQVB and the fact that it can quench both fluorescein and x-rhodamine emission. Normalization of the spectra at the maximum of the donor band eliminates the quenching effect of pMQVB, and the sensitized emission of the acceptor can be observed as shown in Fig. 4B (inset). A small enhancement of the x-rhodamine fluorescence intensity evidences the energy transfer process between the donor/acceptor pair, thus indicating that the interstrand cross-linking of DNA duplexes takes place. The cross-linking efficiency was already reported to be very low [4–6], therefore, the very small spectral changes caused by energy transfer are in accordance with the expectation. Further discussion of the energy transfer data requires, however, examination of the quenching effect of pMQVB on the dsONF and dsONXR spectra.

Titration of single-component systems (ssONF, dsONF, dsONXR) with pMQVB under the same experimental conditions produced a quenching similar to that observed for the ONF/ONXR mixture. The Stern–Volmer plots were linear for all titrations and the calculated Stern–Volmer constants (K_{SV} values) are displayed in Table I. Very high values of K_{SV} can be explained by a local

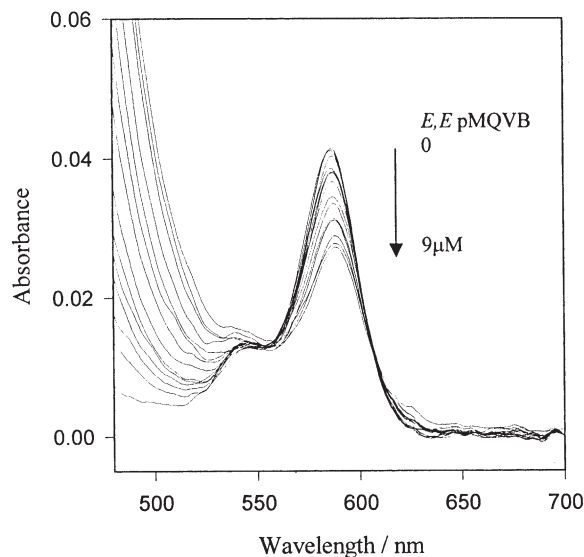


FIGURE 5 Spectrophotometric titration of dsONXR with *E,E* pMQVB. Conditions: [dsONXR] = 0.5 μ M, [pMQVB] = 0–9 μ M, [NaCl] = 200 mM, TE buffer (10 mM, pH 7.8).

accumulation of the quencher in the vicinity of DNA, which is consistent with a high value of the binding constant of *E,E* pMQVB with DNA ($K_b = 1 \times 10^6$) [13]. However, the intercalation cannot exclusively account for the observed quenching since ssONF is also quenched efficiently by the ligand; moreover, ONF duplex with the same base pair sequence as dsONXR is quenched *ca.* three times more efficiently than the latter. Taking into account the limited electrostatic interactions (high salt concentration—200 mM NaCl) between the charged species, one can suppose that the additional specific interactions between pMQVB and the labels occur. Stacking interactions of the planar *E,E* pMQVB with aromatic rings of the label can perturb their electronic systems, and thus can lead to static quenching. Spectrophotometric titrations of the dsONF and dsONXR with pMQVB have been carried out in order to evaluate the extent of such interactions. In both the cases, addition of pMQVB produced gradual changes in the absorption band of the label (hypochromicity and red shift of the band maximum). An example of dsONXR titration spectra is shown in Fig. 5. Such spectral changes are typical of stacking interactions of fluorophores that can result in the formation of non-fluorescent associates responsible for static quenching. To extract the values of the association constants of pMQVB/label complexes, the changes in the absorbance were analyzed in terms of the Benesi–Hildebrandt equation and the values of K_a are shown in Table I. Higher affinity of the fluorescein for complex formation with *E,E* pMQVB seems to be in accordance with the double negative charge borne by the fluorescein molecule at pH 7.8. It should be noted that the values of K_{SV} are at least three times

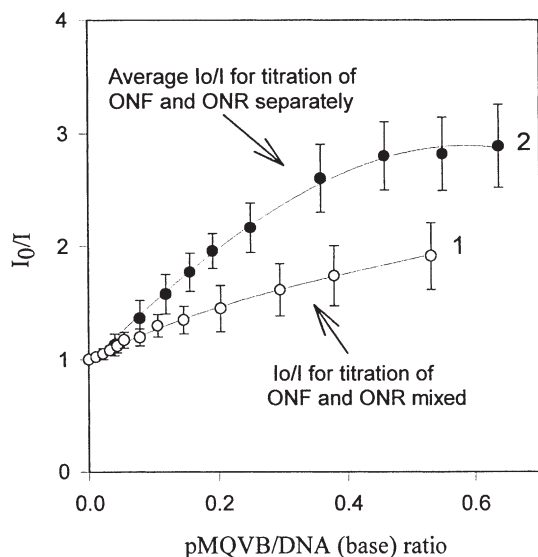


FIGURE 6 The energy transfer between the dsONF/dsONXR couple evidenced by the difference in Stern–Volmer plots for duplex mixture (open circles) and single-component systems (closed circles) titrated with *E,E* pMQVB. Conditions: [dsONF] = [dsONXR] = 0.5 μ M, [*E,E* pMQVB] = 0–9 μ M, [NaCl] = 200 mM, TE buffer (10 mM, pH 7.8). Excitation and emission wavelengths were: 490 and 602 nm for duplex mixture, 490 and 516 nm for ONF, 585 and 602 nm for ONXR.

higher than the corresponding K_a values. This suggests the presence of two quenching mechanisms, a static and a dynamic one (probably electron transfer). In conclusion the energy transfer signal is shielded by a strong quenching effect of pMQVB on the fluorescence of both fluorescein and x-rhodamine. The observed spectral changes depend on the magnitude of these two competing processes.

The extent of FRET can be evaluated from a decrease in the donor emission or from the sensitized fluorescence of the acceptor. Taking into account a low K_{SV} value and a relatively low intensity of the directly excited x-rhodamine emission, we decided to follow FRET using x-rhodamine fluorescence. However, the quenching is much more efficient than the energy transfer, and shields an increase in the sensitized fluorescence of x-rhodamine. The only way to get evidence of the energy transfer occurrence is to compare the experimental quenching dependence with the expected quenching obtained from separately titrated dsONXR. Additionally, the energy transfer spectra contain also the fluorescence of pMQVB and fluorescein that overlap with the x-rhodamine spectrum; therefore, we analyzed the total emission in order to isolate the x-rhodamine spectrum using the method described in the Experimental section. Assuming that there is no energy transfer in the system, both dependencies should overlap within experimental error. On the other hand, the presence of energy transfer adds sensitized emission to the directly excited spectrum of x-rhodamine, therefore, the resulting quenching

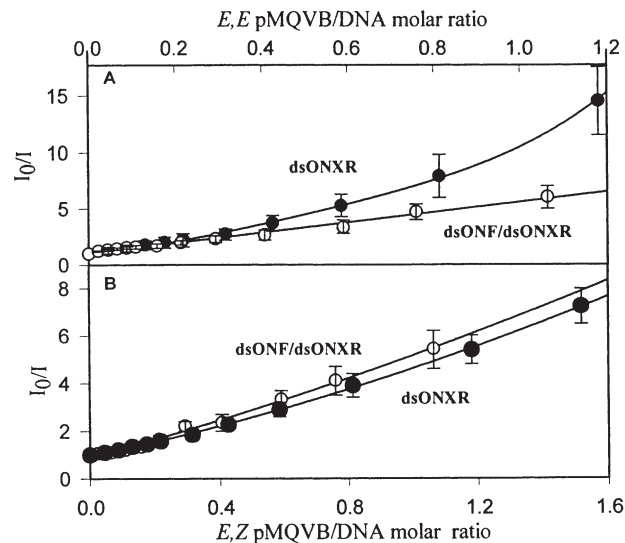


FIGURE 7 The effect of the structure of the cross-linking ligand on the energy transfer between the dsONF/dsONXR couple evidenced by the quenching effect of *E,E* pMQVB (panel A) and *E,Z* pMQVB (panel B). Open circles represent experimental quenching of x-rhodamine emission (isolated from total emission) in duplex mixture and closed circles show quenching of emission of dsONXR alone. Conditions: [dsONF] = [dsONXR] = 0.5 μ M, [pMQVB] = 0–9 μ M, [NaCl] = 50 mM, TE buffer (10 mM, pH 7.8). Excitation wavelengths were 490 and 585 nm for the dsONF/dsONXR mixture and dsONXR, respectively.

should be apparently less efficient. Figure 6 shows the final dependencies of I_0/I vs. pMQVB/DNA ratio. As follows from Fig. 6, the fluorescence quenching for dsONXR (plot 1) is significantly lower than that for dsONF (plot 2) and this difference can be only accounted for by the contribution from the energy transfer process.

To confirm this conclusion, we examined the behavior of the *E,Z* isomer of pMQVB, for which the cross-linking ability should be much lower, if any. One arm of the ligand is in a *cis* conformation (Fig. 1) that protects its quinolinium ring from intercalation to DNA. To ensure a sufficient binding ratio of the ligand to DNA (*E,Z* isomer exhibits a lower DNA binding affinity), titrations were carried out at lower NaCl concentration (50 mM). For reference purposes, the effect of the *E,E* isomer was also studied under these conditions. The obtained Stern–Volmer plots (Fig. 7) showed significant positive curvature typical of quenching by a mixed mechanism of dynamic and static quenching [15]. The values of quenching constants determined from their initial run are displayed in Table I. The lower quenching ability of *E,Z* isomer relative to that of *E,E* form is in good agreement with the higher DNA binding affinity of the latter. A decrease in the concentration of NaCl significantly enhanced the quenching in accordance with the salt concentration effect on the interaction of the oppositely charged species. The dependence for *E,E* isomer also shows a lower quenching for the dsONF/dsONXR system (Fig. 7A) that evidences the

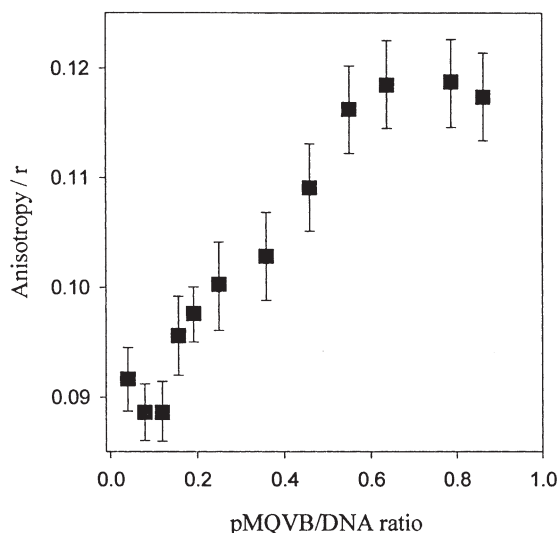


FIGURE 8 Fluorescence anisotropy changes upon titration of dsONXR with *E,E* pMQVB. Conditions: [dsONXR] = 0.5 μ M, [*E,E*pMQVB] = 0–4 μ M, [NaCl] = 200 mM, TE buffer (10 mM, pH 7.8). Excitation wavelength was 585 nm.

energy transfer contribution to the x-rhodamine spectrum. On the contrary, in the case of *E,Z* isomer, both the plots (for dsONXR alone and dsONF/dsONXR mixture) show similar quenching efficiency, which suggests that the ligand in the *E,Z* conformation is unable to effectively cross-link DNA duplexes.

Fluorescence Anisotropy Measurements

The presence of three fluorophores in the energy transfer system (fluorescein, x-rhodamine, and pMQVB) causes some difficulties in resolving particular spectral components from the total emission collected. The fluorescence energy transfer originating from cross-linking of DNA can also occur between like species, e.g. two dsONXR duplexes, provided that the spectral overlap is significant (small Stokes shift) and this phenomenon is called energy migration [16]. Such a process cannot be detected by conventional steady-state measurements, but fluorescence depolarization of fluorophore emission is affected in such cases. Thus, fluorescence anisotropy of the label should undergo particular changes upon titration with the cross-linking agent. This technique has been successfully applied to study DNA–dye complexes [17–19]. The energy transfer (migration) between the bound dyes was reported to cause a decrease in the fluorescence anisotropy with the density of bound dye (separation distance), binding geometry, and unwinding of DNA [19].

An advantage of this method is a decrease in the number of spectral components in the system that simplifies the problem of multicomponent spectra analysis. x-Rhodamine can be excited at the

maximum of its absorption band to reduce the background emission and eliminate the excitation of pMQVB. Moreover, the probability of cross-linking, and thus the energy migration is expected to be higher, which is explained as follows. Assuming that in a three-component system (conventional energy transfer case) there are four spectroscopically active duplexes: fluorescent ONF and ONXR, and non-fluorescent ONFq and ONXRq (q means quenched by pMQVB), one can expect 10 cross-linking products (ONFq–ONFq, ONFq–ONXRq, ONFq–ONF, ONFq–ONXR, ONF–ONF, ONF–ONXRq, ONXRq–ONXRq, ONXRq–ONXR, ONF–ONXR) and only ONF–ONXR is responsible for the energy transfer signal. On the other hand, in a two-component system (anisotropy case), two different duplexes are present: ONXR and ONXRq, thus the expected number of cross-linked pairs is reduced to three (ONXRq–ONXRq, ONXRq–ONXR, ONXR–ONXR) with ONXR–ONXR being responsible for the anisotropy changes. This simple discussion shows clearly the advantages of anisotropy measurements. Additionally, the critical radius calculated for dsONXR was very large, $R_0 = 56 \text{ \AA}$ (for $\kappa^2 = 2/3$, $n = 1.36$, $\epsilon^{586} = 8.9 \times 10^4 \text{ M}^{-1} \text{ cm}^{-1}$, and $\phi^{\text{ONR}} = 0.5$). The anisotropy changes measured upon titration with pMQVB are presented in Fig. 8. The anisotropy slightly decreases at a low ligand concentration, then increases with the cross-linking ligand concentration, and finally reaches saturation at a *D/P* ratio (dye to DNA phosphate molar ratio) of about 0.6. Generally, the anisotropy depends on the rotational diffusion that the excited molecule undergoes before it emits a photon. Two types of rotation contribute to the depolarization process, the rotation of the fluorescent label about the linkage that connects it with DNA, and the rotation of the macromolecule as a whole. In the absence of a cross-linking agent, the anisotropy is quite low ($r = 0.09$), which suggests efficient rotational depolarization, probably due to both processes. The contribution coming from the free rotation of a relatively short duplex (8-mer) could be quite high. For example, McLaughlin *et al.* reported values of r in the range of 0.26–0.35 for fluorescein- and eosin-labeled 24-mers [20], which may suggest an increase in the anisotropy as a result of an increase in molecular weight of the macromolecule. The cross-linking of two duplexes may have a two-fold effect on the anisotropy: on one hand, it can reduce the anisotropy due to homo energy transfer, and on the other, anisotropy can increase because of a slower rotation of a larger cross-linked macromolecule. As the binding ratio of pMQVB increases, larger aggregates may be formed (three, four, etc. cross-linked duplexes) slowing down the rotation. An explanation of the observed dependence should take into regard the two processes responsible for the



FIGURE 9 Dynamic fluorescence microscopy freeze frames of Bacteriophage T4 DNA in the absence (panel A), and in the presence of 0.1 μM (panel B) and 1 μM of *E,E* pMQVB (panel C). Conditions: [T4DNA] = 0.1 μM , [DAPI] = 0.1 μM , TB buffer (10 mM, pH 8.0). Excitation wavelength was 380 nm.

depolarization of fluorescence. The initial decrease can be interpreted as the depolarization caused by the energy transfer process and this effect is overwhelmed next by restriction in the rotational depolarization of the cross-linked duplexes.

Fluorescence Microscopy Imaging

It has been shown that dynamic information on the higher-order structure of DNA can be obtained for individual DNA molecules in aqueous environment using fluorescence microscopy and an appropriate fluorescence dye [21,22]. The well known DNA groove binder, 4,6'-diamidino-2-phenylindole (DAPI), is widely used for such visualization of DNA, since it does not affect the contour length of DNA upon binding, contrary to common intercalating ligands [22]. We decided to use this technique to get another solid proof of the cross-linking. Figure 9 shows typical freeze-frame fluorescence images (converted to black and white pictures) of T4 DNA molecules obtained in the absence and the presence of cross-linking ligand pMQVB. The untreated T4 DNA (Fig. 9A) occurs in the form of a string-like aggregate with the apparent contour

length exceeding 5 μm . The extended conformation or coiled state is typical of the DNA molecule that exhibits translational and intramolecular Brownian motions. The addition of pMQVB (0.1 μM) induces the formation of globular-type particles (Fig. 9B), a further increase in pMQVB concentration (1 μM) causes an increase in the number of globular particles and a slight compaction of these globules (Fig. 9C). The explanation of the observed effect should involve the interaction of the DNA molecule with the bisintercalator added. The probability of cross-linking of two T4 DNA molecules seems to be very low in this system in view of the low DNA concentration (0.1 μM nucleotides) and unfavorable entropic factor. Therefore, the effects observed should be explained by the changes in the higher-order structure of T4 DNA molecules. Upon addition of the cross-linking bisintercalator, the coiled T4 DNA molecule is cross-linked through space yielding globular species. Although the ligand intercalates to the same DNA molecule (intrastrand), this process can be regarded as an intermolecular cross-linking because two remote parts of the DNA molecule are connected. The compaction of globules at a higher ligand concentration may suggest involvement of several bisintercalators in the cross-linking of the same DNA molecule. The efficiency of cross-linking can be estimated from Fig. 10 that shows the effect of pMQVB concentration on the long-axis length of T4 DNA. At a very low ligand concentration, DNA molecules remain in the extended coil state; the size distribution has a mean value of 7 μm and a standard deviation of 0.6 μm , indicating a fluctuation of the conformation. The length of the DNA molecule becomes shorter when the ligand/nucleotide ratio approaches 1 and decreases with ligand concentration. Finally, the size distribution reaches saturation at a D/P ratio of about 10 with a mean value of 4.5 μm and a broader standard deviation of 1.1 μm .

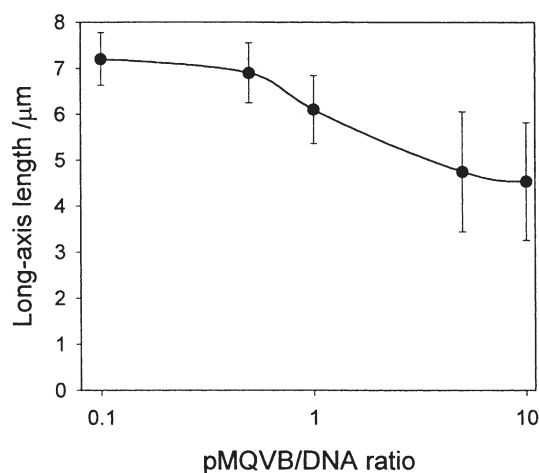


FIGURE 10 Changes of the long-axis length of T4DNA depending on the pMQVB/DNA concentration ratio under the conditions described in Fig. 9. At least 30 DNA molecules were analyzed for each pMQVB concentration. Error bars indicate the standard deviation in the distribution.

CONCLUSIONS

The rigid intercalator, 1,4-bis((*N*-methylquinolinium-4-yl)vinyl)benzene, is able to cross-link DNA

duplexes, which was evidenced by the results of FRET, fluorescence anisotropy measurements, and dynamic fluorescence microscopy. The energy transfer takes place only in the presence of the planar *E,E* isomer, thus suggesting the importance of bisintercalation process in the cross-linking. The *E,Z* isomer appeared to be a poor cross-linking agent in accordance with its non-planar structure (one arm of the ligand in a *cis* configuration).

The results presented showed that FRET can be applied for the investigation of cross-linking of DNA, and although the quenching properties of the bisintercalator may shield the sensitized emission of the acceptor, a careful analysis of the experimental data can provide some evidence of energy transfer. The dynamic fluorescence microscopy showed the ability of the ligand to alter the higher-order structure of large DNA molecules, thus confirming the cross-linking abilities of pMQVB. The demonstration that the ligand induces a compaction of DNA suggests that small molecules (bisintercalators) can be useful to control gene expression through alteration of the higher-order structure of DNA. Such ligands could also affect the processes requiring the presence of two duplexes in a close proximity, e.g. recombination and replication of DNA, or topoisomerase action.

EXPERIMENTAL

Materials

Bacteriophage T4 DNA (166 kbs, 57 μ m contour length) was purchased from Nippon Gene (Tokyo, Japan). Three 8-mer deoxyribonucleotides used in the FRET studies were synthesized and HPLC-purified by TaKaRa, (Tokyo, Japan). The octamer 5'-CGTACGGC-3' was single-labeled at the 5' end with fluorescein isothiocyanate (ONF) or x-rhodamine isothiocyanate (ONXR) via a 6-carbon spacer. An unlabeled oligomer 5'-GCCGTACG-3' (ON) was used as a complementary strand to obtain double-stranded DNA. Concentrations of oligomers were determined using molar absorptivities calculated from the contributions of both DNA and label. The contribution of label absorbance at 260 nm was assumed to be 19% of the absorbance of long-wavelength band of the labels. The molar absorptivities for DNA strands were calculated by the nearest-neighbor method, from published values of molar absorptivities for monomer and dimer DNA [23]. The final values of molar absorptivities (ϵ) used for quantitation of ON, ONF, and ONXR were 7.5×10^4 , 8.5×10^4 , and $9.1 \times 10^4 \text{ M}^{-1} \text{ cm}^{-1}$, respectively. Fluorescein and x-rhodamine labeled duplexes (dsONF and dsONXR, respectively) were obtained by incubation of preliminary heated (65°C) 1:1

mixture of labeled and unlabeled complementary strands at 10°C for 30 min.

1,4-Bis((*N*-methylquinolinium-4-yl)vinyl)benzene ditriflate (*E,E* pMQVB) was prepared by the reaction of methyl trifluoromethanesulfonate with 1,4-bis((quinolin-4-yl)vinyl)benzene that was obtained by the known procedure [24].

m.p. > 300°C. NMR (250 MHz, DMSO- d_6): δ_{H} 4.58 (6H, s, N^+Me), 8.23 (2H, d, $J = 16 \text{ Hz}$, *trans* H-vinyl), 8.51 (2H, d, $J = 15.7 \text{ Hz}$, *trans* H-vinyl). Anal. Found: C, 54.19; H, 3.67; N, 4.15%. Calcd for $\text{C}_{32}\text{H}_{26}\text{N}_2\text{O}_6\text{F}_6\text{S}_2$: C, 53.90; H, 3.68; N, 3.93%.

The *E,Z* isomer of pMQVB was prepared by the HPLC separation of the mixture of *E,E* and *E,Z* isomers obtained under irradiation of the *E,E* pMQVB.

Tris-HCl, DAPI, and the antioxidant 2-mercaptoethanol (ME) were obtained from Wako Pure Chemical Industries (Osaka, Japan). All the experiments were conducted in TE buffer pH = 7.8 (10 mM Tris-HCl, 1 mM EDTA). Sodium chloride was added to obtain the desired salt concentration (200 or 50 mM). Milli-Q filtered water (Millipore, Bedford, MA) was used throughout.

Methods

^1H NMR spectra were recorded on a Bruker spectrometer operating at 250 MHz using tetramethylsilane as an internal standard. Absorption spectra were obtained with a Hitachi U-3300 spectrophotometer equipped with a SPR 10 temperature controller. Steady-state fluorescence measurements were carried out using a Hitachi F-4500 spectrofluorimeter with 5 nm excitation and emission slits. The cell compartment was thermostated at 10°C and equipped with a magnetic stirrer. All measurements were carried out using a 10 mm quartz cell, the spectra were corrected in 280–700 nm range by a microprocessor-operated correction mode, using Rhodamine B as a photon counter.

Melting Curves

Melting of duplexes was followed by conventional absorbance measurements at 260 nm with controlled temperature gradient. Samples in TE buffer (200 mM NaCl) containing the mixture (0.5 μ M each strand) of labeled (ONF or ONXR) and unlabeled complementary oligonucleotide (ON) were initially incubated at 5°C for 20 min, slowly heated to 65°C (at 1°C min^{-1}) and next slowly cooled to 10°C. Both cooling and heating cycles gave almost reproducible runs.

Spectrophotometric Titration

A sample solution containing 0.5 μ M of duplex (dsONF or dsONXR), TE buffer (pH 7.8), and

200 mM NaCl was equilibrated at 10°C for 10 min. A typical titration consisted of successive addition of small portions (5 μ l) of a 50 μ M solution of pMQVB that contained buffer, NaCl, and duplex (at the same concentration as in the sample), followed by stirring, thermal equilibration, and recording of the spectrum. The absorbance changes at the maximum wavelength of the absorption band of the label were analyzed using Benesi–Hildebrand transformation [25] to obtain the association constant (K_a) of the complex formed, from the following equation:

$$\frac{[\text{DNA}]}{\Delta A} = \frac{1}{\Delta \epsilon} + \frac{1}{K_a \Delta \epsilon c_L},$$

where $\Delta \epsilon$ is the difference between molar absorptivities of free and complexed DNA label, c_L is the titrant (pMQVB) concentration.

Fluorescence Titration and Energy Transfer Measurements

A sample solution containing dsONF and dsONXR (0.5 μ M each), TE buffer, and NaCl (50 or 200 mM) was equilibrated in a quartz cell at 10°C for 10 min. After successive additions (5 μ l) of a 50 μ M solution of pMQVB (containing the same components as the sample including duplexes), stirring, and thermal equilibration, the fluorescence emission spectra were recorded in the 500–700 nm range with an excitation wavelength of 490 nm (dsONF/dsONXR mixture, dsONF alone) and 580 nm (dsONXR). The spectra were recorded using a set of polarizers aligned at the “magic angle.” Experimental emission spectra were resolved using the multicomponent analysis method to extract the x-rhodamine spectrum. The calculations were performed using PhotochemCAD software that allows a quantitative multicomponent analysis of a spectrum composed of several different components [26]. Quenching effect and energy transfer efficiency were evaluated using plots of I_0/I vs. D/P ratio.

Anisotropy Measurements

A sample solution of dsONXR (0.5 μ M) was titrated with pMQVB similar to other titration procedures. Emission spectra were recorded over the wavelength range 585–700 nm (excitation wavelength 580 nm) using a set of polarizing filters. Anisotropy, r , was calculated from the following equation: $r = \frac{I_{VV} - I_{VH}G}{I_{VV} + 2I_{VH}G}$ where $G = \frac{I_{HV}}{I_{HH}}$, I is integrated fluorescence, subscripts V and H represent vertical and horizontal settings of polarizers. The first index denotes excitation, the second—emission polarizer. G is used for instrumental correction.

Fluorescence Microscopy

A sample solution containing T4 DNA (0.1 μ M nucleotides), fluorescence dye DAPI (0.1 μ M),

antioxidant ME (4%) in TE buffer pH 7.8 were mixed with pMQVB and equilibrated at 25°C for 15 min. The sample solution was placed between microscope slides, illuminated with 365 nm UV light, and fluorescence images of DNA molecules were observed using a Zeiss Axiovert 135 TV microscope equipped with a 100 \times oil-immersed objective lens, and recorded on a S-VHS videotape through a high-sensitivity Hamamatsu SIT TV camera.

Acknowledgments

The present study was partially supported by the Grant in Aid for Scientific Research from the Japan Ministry of Education, Science, and Culture.

References

- [1] LePecq, J.-B., Le Bret, M., Barbet, J. and Roques, B. (1975), *Proc. Natl Acad. Sci. USA* **72**, 2915.
- [2] King, H.D., Wilson, W.D. and Gabbay, E.J. (1982), *Biochemistry* **21**, 4982.
- [3] Welsh, J. and Cantor, C.R. (1987), *J. Mol. Biol.* **198**, 63.
- [4] Huang, C.-H., Mirabelli, C.K., Mong, S. and Crooke, S.T. (1983), *Cancer Res.* **43**, 2718.
- [5] Mullins, S.T., Annan, N.K., Cook, P.R. and Lowe, G. (1992), *Biochemistry* **31**, 842.
- [6] Annan, N.K., Cook, P.R., Mullins, S.T. and Lowe, G. (1992), *Nucleic Acids Res.* **20**, 983.
- [7] Morrison, L.E., Halder, T.C. and Stols, L.M. (1989), *Anal. Biochem.* **183**, 231.
- [8] Clegg, R.M., Murchie, A.I.H., Zechel, A., Carlberg, C., Diekmann, S. and Lille, D.M.J. (1992), *Biochemistry* **31**, 4846.
- [9] Mergny, J.-L., Boutorine, A.S., Garestier, T., Belloc, F., Rougee, M., Bulychev, N.V., Koshkin, A.A., Bourson, J., Lebedev, A.V., Valeur, B., Thuong, N.T. and Helene, C. (1994), *Nucleic Acids Res.* **22**, 920.
- [10] Parkhurst, K.M. and Parkhurst, L.J. (1995), *Biochemistry* **34**, 285.
- [11] Juskowiak, B., Ohba, M., Sato, M., Takenaka, S., Takagi, M. and Kondo, H. (1999), *Bull. Chem. Soc. Jpn* **72**, 265.
- [12] Juskowiak, B., Takenaka, S. and Takagi, M. (1999), *Chem. Lett.*, 209.
- [13] Juskowiak, B., Galezowska, E. and Takenaka, S., *Spectrochim. Acta P.A.*, in press.
- [14] Juskowiak, B., Ichihara, T., Takenaka, S. and Takagi, M. (2001), *Pol. J. Chem.* **75**, 1377.
- [15] Zeng, H. and Durocher, G. (1995), *J. Lumin.* **63**, 75.
- [16] Lakowicz, J.R. (1983) *Principles of Fluorescence Spectroscopy* (Plenum Press, New York), p 111.
- [17] Paoletti, J. and LePecq, J.B. (1971), *J. Mol. Biol.* **59**, 43.
- [18] Barcelona, M.L. and Gratton, L. (1996), *Biophys. J.* **70**, 2341.
- [19] Carlsson, C., Larsson, A., Bjorkman, M., Jonsson, M. and Albinsson, B. (1997), *Biopolymers* **41**, 481.
- [20] McLaughlin, L.W. and Ozaki, H. (1992), *Nucleic Acids Res.* **20**, 5205.
- [21] Yoshikawa, K., Matsuzawa, Y., Managawa, K., Doi, M. and Matsumoto, M. (1992), *Biochem. Biophys. Res. Commun.* **88**, 1274.
- [22] Matsuzawa, Y. and Yoshikawa, K. (1994), *Nucleosides Nucleotides* **13**, 1415.
- [23] Fasman, G.D., (1975) In: *CRC Handbook of Biochemistry and Molecular Biology Nucleic Acids*, 3rd ed. (CRC Press, Cleveland, Ohio) **Vol. 1**, p 589.
- [24] Kunitake, M., Nasu, K., Manabe, O. and Nakashima, N. (1994), *Bull. Chem. Soc. Jpn* **67**, 375.
- [25] Benesi, H. and Hildebrand, J.H. (1949), *J. Am. Chem. Soc.* **71**, 2703.
- [26] Du, H., Fuh, R.-C.A., Li, J., Corkan, L.A. and Lindsey, J.S. (1998), *Photochem. Photobiol.* **68**, 141.